2009 American Control Conference
Hyatt Regency Riverfront, St. Louis, MO, USA
June 10-12, 2009

Modular Discrete Optimal MIMO Controller for a VCT Engine

Melih Çakmakcı and A. Galip Ulsoy

***Abstract*— In early computer control, only one centralized computer was responsible for executing the algorithms for a particular system. Increasingly, computer control algorithms reside inside individual system components in a distributed fashion. Variable Camshaft Timing (VCT) is an appealing feature for automotive engines because it allows optimization of the cam timing over a wide range of operating conditions. In this paper, a method to distribute the discrete MIMO controller for the VCT Engine to improve the component swapping modularity of the VCT Actuator and the EGO Sensor components using network communications is presented. First a discrete LQG controller was designed then this controller was distributed to the ECU, the VCT controller and the EGO sensor controller in order to improve the component swapping modularity of the system. A control oriented *pre-optimization* technique, which simplifies the optimization problem and a candidate solution was devised to maximize component modularity.**

I. Introduction

Although in the early days of computer control, only one centralized computer was responsible for executing the algorithms for a particular system, increasingly, computer control algorithms reside inside individual system components in a distributed fashion. For example, there are up-to 80 microcontrollers in today's high-end vehicles and it is expected that by 2010, 90% of all computer code will reside in such embedded systems [1].

As control systems are implemented in an increasingly distributed fashion, modularity of the overall system becomes an important design decision. Ulrich and Tung [2] define modularity in terms of two characteristics of product design: (1) Similarity between the physical and functional architecture of the design and (2) Minimization of incidental interactions between physical components. They also state that "*component-swapping modularity occurs when two or more alternative basic components can be paired with the same modular components creating different product variants belonging to the same product family*".

Fig. 1 describes physical and functional boundaries for a networked control system with bi-directional communications and smart components. When a component change occurs (sensor or actuator shown in Fig. 1-a) both overall controller (Fig. 1-b) and overall plant dynamics (Fig. 1-c) are affected. Control systems with modularly swappable components can then be defined as systems in which the initial and final configurations due to a component change operate at their corresponding optimal performance. By using the additional design freedom, with networked control systems with bi-directional communications, it is possible to improve component swapping modularity of the system by containing the plant dynamics and corresponding control algorithm changes only in the affected components physical boundaries [3], [4].

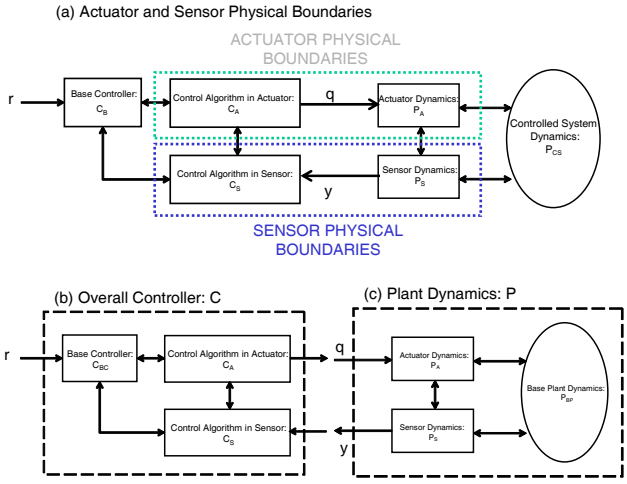

Fig. 1. Control System Component Physical and Functional Boundaries.

Variable Camshaft Timing (VCT) is an appealing feature for automotive engines because it allows optimization of the cam timing over a wide range of operating conditions [5]. VCT schemes not only improve fuel economy [6], [7], [8], but also reduce emissions [9], [10] while improving full load performance [11].

VCT schemes increase internal residual gas by affecting the intake, combustion and exhaust phases of the engine cycle. Increase in internal residual gas reduces the combustion temperature which decreases nitrogen oxide, NO_x, formation. The internally recirculated exhaust gas is rich in unburned hydrocarbons, HC, which can be burned in the next cycle. Application of VCT schemes, since they require higher manifold pressure, decrease pumping losses which results in improved fuel economy. However, dilution of the in-cylinder mixture adversely affects the engine torque response. These factors define the trade-off between good emissions and good drivability for VCT engines. In [12], the detailed operation of a continuous variable cam timing component is described. This variable camshaft timing system works on the principle of sliding helical gears controlled by a hydraulic piston.

In this paper, we present the design and distribution of a discrete MIMO controller for a variable camshaft timing (VCT) engine. The resulting distributed controllers maximize

Melih Çakmakcı (cakmakci@umich.edu) and A. Galip Ulsoy are with the Department of Mechanical Engineering, University of Michigan, Ann Arbor, MI, 48109-2125, USA.

the component swapping modularity of the *smart* VCT Unit and *smart* EGO Sensor. In the next section, the VCT engine model used in the controller design and the discrete MIMO controller design will be presented. Next, distribution of the controller design to engine control unit (i.e. ECU), VCT Controller and EGO controller to maximize component-swapping modularity will be discussed. Subsequently, we present our conclusions and research plan for future steps in the last section.

II. Engine Modeling and MIMO Control Design

A. VCT Engine Model

The development of a continuous, non-linear, low-frequency, phenomenological and control oriented VCT engine model was discussed in [13] based on the model structure given in [14] and other references. The input/output relationship of the plant model developed is given in Fig. 2.

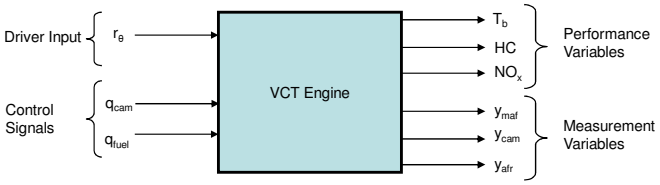

Fig. 2. Input Output relationship of the dynamic plant model for control development.

In previous work an experimental setup was used to develop relationships for the engine breathing process, torque generation and feedgas HC and NO_x emissions were developed. Details of this work will not be discussed here, and the reader is referred to [13] and [5].

B. Dynamics of the VCT Unit and EGO Sensor

In order to model the VCT actuator dynamics, a first order transfer function where $\tau_{v,a} = 0.0371$ will be used:

$$Y_{c,act}(s) = \frac{-0.013s + \tau_{v,a}}{s + \tau_{v,a}} Q_c(s) \tag{1}$$

where Q_c is the commanded cam phase angle. The non-minimum phase zero observed in Eqn. (1) is an artifact of the identification process.

For the VCT sensor, a delay of two fundamental sampling periods was assumed, modeled as a first order Pade approximation with parameter $\tau_{v,s}$. For an n cylinder engine at a speed of N rpm the fundamental sampling rate is defined as [13]:

$$\Delta T = \frac{120}{Nn} \tag{2}$$

The dynamics of the EGO sensor is modeled as first order with a time constant $\tau_e = 70$ms:

$$Y_{afr}(s) = \frac{1/\tau_e}{s + 1/\tau_e} Y_{afr,exh}(s) \tag{3}$$

The Matlab/Simulink plant model for the VCT engine was developed based on the information and regression data given in [13]. The response of the overall model was then validated using loop model results in [13], [15].

C. Discrete-time MIMO Controller Design

The dynamic engine model described in the previous section is linearized around the nominal inputs, i.e CAM Angle $= 10°$, Fuel $= 0$ grams and Throttle Angle $= 9.33°$, and the corresponding steady state internal states using Matlab/Simulink.

The linearized model is then discretized with a sampling period ΔT to obtain

$$\mathbf{x}(k+1) = \mathbf{A_d}\mathbf{x}(k) + \mathbf{B_d}\mathbf{u}(k) + \mathbf{B_{r1,d}} r_\theta(k) \tag{4}$$

$$\mathbf{y}(k) = \mathbf{C_d}\mathbf{x}(k) + \mathbf{D_d}\mathbf{u}(k) + \mathbf{B_{r1,d}} r_\theta(k) \tag{5}$$

where

$$\mathbf{A}_d = \begin{bmatrix} \mathbf{A}_{d1} & \mathbf{A}_{d2} \end{bmatrix}$$

$$\mathbf{A}_{d1} = \begin{bmatrix} 0.8984 & -0.01638 & 0.02042 & 0.0025 & 0.0003 \\ 0 & 0.8169 & 0 & 0 & 0 \\ 0 & 0.1153 & 0.3679 & 0 & 0 \\ 0 & -0.00107 & 0.0307 & 0.9435 & 0.022 \\ 0 & 0 & 0 & 0 & 0.7575 \\ 0 & 0.0045 & 0 & 0 & 0 \\ 0 & 1e-6 & -7e-5 & 0.0002 & 1e-5 \\ 0 & -0.0238 & -0.0032 & 0.0456 & 0.0054 \\ 0 & -7e-5 & -0.0003 & 0.0005 & 5e-5 \end{bmatrix}$$

$$\mathbf{A}_{d2} = \begin{bmatrix} 0.1543 & -656.314 & -0.8944 & 10.1589 \\ 0 & 0 & 0 & 0 \\ 0 & 0 & 0 & 0 \\ 0 & 0 & 0 & 0 \\ 0 & 0 & 0 & 0 \\ 0.944 & 0 & 0 & 0 \\ 0 & 0.3679 & 0 & 0 \\ 0.2551 & -1240 & 0.466 & -14.0665 \\ 0.0011 & -6.3646 & 0.0053 & 0.9407 \end{bmatrix}$$

$$[\mathbf{B}_{r1,d}, \mathbf{B}_d] = \begin{bmatrix} 0.00038175 & -5.354e-5 & 0.14931 \\ 0 & 0.0067904 & 0 \\ 0 & 0.00046453 & 0 \\ 0.00024734 & -7.5544e-6 & 0 \\ 0.018606 & 0 & 0 \\ 0.0024429 & 1.5316e-5 & 0 \\ 2.2866e-7 & 2.2808e-8 & 0.0047409 \\ 0.00052672 & -6.6406e-5 & 1.4671 \\ 1.5265e-6 & -1.3251e-7 & 0.014705 \end{bmatrix}$$

$$\mathbf{C}_d = \begin{bmatrix} 14.2857 & 0 & 0 & 0 & 0 & 0 & 0 & 0 & 0 \\ 0 & -27.310 & 266.667 & 0 & 0 & 0 & 0 & 0 & 0 \end{bmatrix}$$

$$\mathbf{D}_d = \begin{bmatrix} 0 & 0 & 0 \\ 0 & 0.013 & 0 \end{bmatrix}$$

Since maintaining the stoichiometric air fuel ratio, and zero steady state error in cam timing, is important during throttle angle changes, integral control of the plant outputs is implemented. This is done by augmenting the state vector with the integral of the output tracking errors:

$$\hat{\mathbf{x}}(k+1) = \begin{bmatrix} \mathbf{A_d} & \mathbf{0} \\ \Delta T \mathbf{C_d} & \mathbf{I} \end{bmatrix} \begin{bmatrix} \mathbf{x}(k) \\ \mathbf{x_I}(k) \end{bmatrix} + \begin{bmatrix} \mathbf{B_d} \\ -\Delta T \mathbf{C_d} \end{bmatrix} \mathbf{u}(k)$$

$$+\begin{bmatrix} \mathbf{B_{r1,d}} & \mathbf{0} \\ \mathbf{0} & -T_s\mathbf{I} \end{bmatrix} \begin{bmatrix} r_\theta(k) \\ r_{cam}(k) \\ r_{afr}(k) \end{bmatrix} \quad (6)$$

By using the discrete-time linear system above an LQR controller with the state feedback gains, K_d was obtained:

$$\mathbf{K}_d^T = \begin{bmatrix} -0.00029813 & -0.013001 \\ 22.2911 & 0.0006195 \\ 126.643 & -0.0087846 \\ 2.84e-5 & 0.025793 \\ -2.79e-6 & 0.0030435 \\ -0.00010603 & -0.038505 \\ 1.6371 & 65.1827 \\ -0.00029203 & -0.0079145 \\ -0.065519 & -2.647 \\ 0.0001704 & 0.0085496 \\ -40.1194 & 0.00095088 \end{bmatrix} \quad (7)$$

Since the only measurements available are the cam timing measurement and the air-fuel measurement, a Kalman Filter is designed to estimate the remaining states with the gains:

$$\mathbf{L}_d = \begin{bmatrix} 0.095152 & 8.486e-5 \\ -9.9756e-11 & 0.00020019 \\ -1.8683e-11 & 0.0014151 \\ -2.6077e-8 & 0.00012182 \\ -1.0599e-10 & -4.7379e-15 \\ 2.8741e-8 & 1.495e-005 \\ -9.9113e-7 & -2.9073e-7 \\ -0.015256 & -6.9183e-6 \\ 0.00014419 & -1.3294e-6 \end{bmatrix} \quad (8)$$

The closed loop system with the discrete MIMO controller is given in Fig. 4. The resulting closed loop (i.e. discrete controller + nonlinear plant model) response to a throttle profile is shown in Fig. 3.

III. Distribution Problem

The block diagram representing the plant and controller relationship for the discrete-time MIMO controller in the previous section is given in Fig. 4. With the controller distribution problem our aim is to find component controllers, $\mathbf{C}_{ecu}$, $\mathbf{C}_v$, $\mathbf{C}_e$ which improve the component swapping modularity of the system by using bi-directional network communications. The block diagram of the proposed distributed system with the proposed communication is given in Fig. 5.

A generic optimization problem formulation for maximizing the component swapping modularity of an actuator component was given in [4]. Given nominal settings for the plant parameters (denoted as $\mathbf{p}_{cs}^0$, $\mathbf{p}_v^0$, $\mathbf{p}_e^0$ for the controlled system i.e., rest of the engine, VCT component and EGO sensor, respectively), we can formulate the distribution problem which maximizes VCT component swapping modularity, M_v while the distribution constraint, desired overall controller must be equal to the overall effect of the distributed controller (i.e $C_{des} = C_{dis}$) holds.

In short, M_v represents the size of the region in the parameter space, which includes the nominal VCT parameters, for

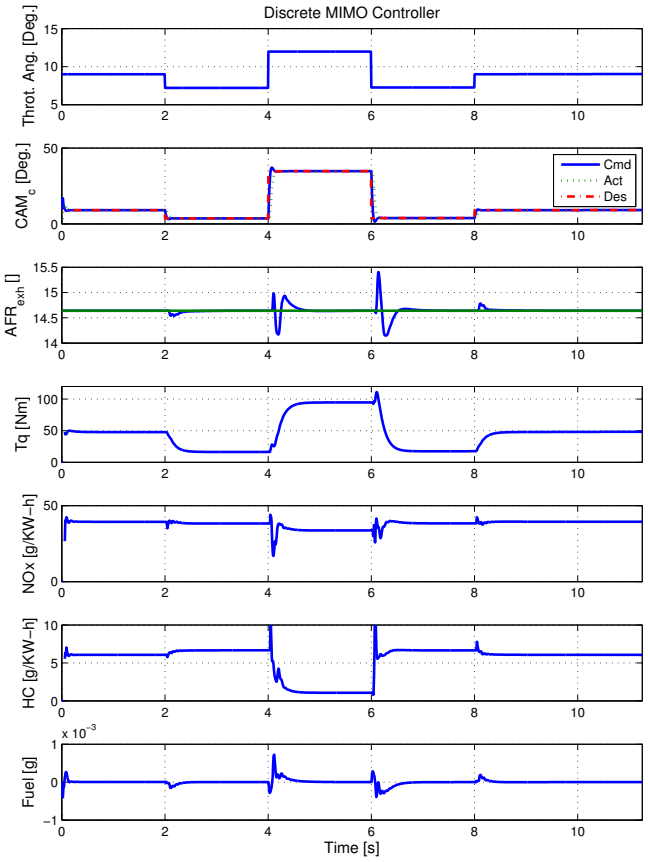

Fig. 3. VCT Engine with Discrete MIMO Controller closed loop response

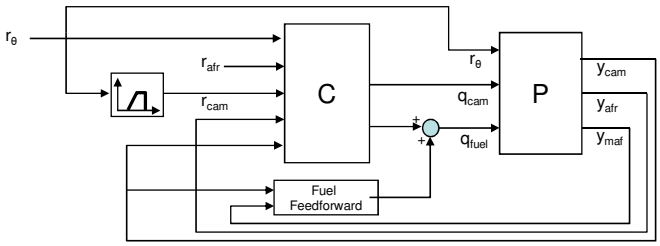

Fig. 4. VCT Engine with Discrete MIMO Controller

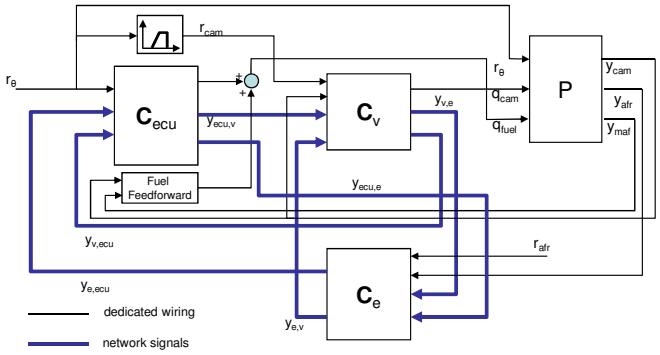

Fig. 5. VCT Engine with Distributed Discrete MIMO Controller

which we can ensure the distribution constraint, by changing only gains of the VCT controller.

A. Formulation of $\mathbf{C}_{des}$

In this section, the formulation for the desired centralized controller, C_{des}, given plant parameters $\mathbf{p}_{cs}^0$, $\mathbf{p}_v^0$, $\mathbf{p}_e^0$ is presented. Given the optimal state feedback matrix $\mathbf{K}_d = [\mathbf{K1}_d, \mathbf{K2}_d]$ and linear observer gain $\mathbf{L}_d$, the state space representation of the discrete MIMO controller in Fig. 4 can be given as

$$\begin{aligned}\mathbf{x}_c(k+1) &= \mathbf{Ac}_d \begin{bmatrix} \mathbf{x}_c \\ \mathbf{x}_{c,I} \end{bmatrix}(k) + \mathbf{Bc}_d\mathbf{u}(k) \\ &\quad + \mathbf{Bc}_{\mathbf{d,r}} \begin{bmatrix} r_\theta \\ r_{cam} \\ r_{afr} \end{bmatrix}(k) \end{aligned} \tag{9}$$

$$\mathbf{q}(k) = \mathbf{C}_d \begin{bmatrix} \mathbf{x}_c \\ \mathbf{x}_{c_I} \end{bmatrix}(k) \tag{10}$$

where

$$\mathbf{Ac_d} = \begin{bmatrix} \mathbf{A_d - L_dC_d - B_dK1_d + L_dD_dK1_d} & \mathbf{L_dD_dK2_d - B_dK2_d} \\ \mathbf{0} & \mathbf{I} \end{bmatrix} \tag{11}$$

$$\mathbf{Bc_d} = \begin{bmatrix} \mathbf{L_d} \\ -T_s\mathbf{I} \end{bmatrix} \tag{12}$$

$$\mathbf{Bc_{d,r}} = \begin{bmatrix} \mathbf{Br_d - L_dDr_d} & \mathbf{0} \\ \mathbf{0} & T_s\mathbf{I} \end{bmatrix} \tag{13}$$

$$\mathbf{Cc_d} = \begin{bmatrix} -\mathbf{K1_d} & -\mathbf{K2_d} \end{bmatrix} \tag{14}$$

We compute the z-transform equivalent transfer function matrix for the discrete state space system given in Equations 9-10 in the form

$$\mathbf{C} = \begin{bmatrix} N_{11}(z)/D_{11}(z) & \cdots & N_{15}(z)/D_{15}(z) \\ N_{21}(z)/D_{21}(z) & \cdots & N_{25}(z)/D_{25}(z) \end{bmatrix} \tag{15}$$

N_{11} and D_{11} are polynomials with vectors $\mathbf{x}_{n11}$ and $\mathbf{x}_{d11}$ of controller gains (Eqn. (16)) respectively,

$$\begin{aligned} C_{11}(\mathbf{x_{n11}}, \mathbf{x_{d11}}, z) &= \frac{N_{11}(\mathbf{x_{n11}}, z)}{D_{11}(\mathbf{x_{d11}}, z)} = \\ &\frac{x_{n11,m}z^{m+1} + ... + x_{n11,n+2}z + x_{n11,n+1}}{x_{d11,n}z^{n+1} + ... + x_{d11,2}z + x_{d11,1}} \end{aligned} \tag{16}$$

Then we can define $C_{des}(\mathbf{p}_v, \mathbf{p}_e, \mathbf{p}_{ecu})$ as

$$\begin{aligned} &C_{des}(\mathbf{p}_v, \mathbf{p}_e, \mathbf{p}_{cs}) = \\ &\quad C(\{\mathbf{x}_{nij}^*, \mathbf{x}_{dij}^* | i = 1, 2; j = 1, 2, ..., 5\}) \end{aligned} \tag{17}$$

where $\{\mathbf{x}_{nij}^*, \mathbf{x}_{dij}^* | i = 1, 2; j = 1, 2, ..., 5\} = argmin\ J_C(P, \mathbf{C}) = \Sigma_1^\infty (x(k)'Qx(k) + u(k)'Ru(k))$ s.t. $\mathbf{x}(k+1) = \mathbf{A}_d\mathbf{x}(k) + \mathbf{B}_d\mathbf{u}(k)$.

The $\mathbf{p}_{cs}$, $\mathbf{p}_v$, $\mathbf{p}_e$ are parameter vectors representing the controlled system (rest of the engine), VCT component and EGO sensor parameters respectively. These polynomial constants vary as VCT and EGO plant parameters change and can be implemented in the numerical solution phase of the problem as lookup tables or regression equations.

B. Formulation of $\mathbf{C}_{dist}$

For the control system given in Fig. 5 and with an a real-time distributed controller schedule which assumes perfect completion of the communication schedule, discrete MIMO equations to calculate the overall controller equation can be written to obtain the equation given in (18).

$$\begin{aligned} \mathbf{C}_{dist}(z) = &- \begin{bmatrix} C_{v13} & 0 & 0 & 0 & 0 & C_{v14} \\ 0 & 0 & 0 & C_{ecu13}/z & C_{ecu12} & 0 \end{bmatrix} \\ &\begin{bmatrix} -1 & 0 & 0 & C_{ecu23}/z & C_{ecu22} & 0 \\ 0 & -1 & 0 & C_{ecu33}/z & C_{ecu32} & 0 \\ C_{v23} & 0 & -1 & 0 & 0 & C_{v24} \\ C_{v33} & 0 & 0 & -1 & 0 & C_{v34} \\ 0 & C_{e14}/z & C_{e13}/z & 0 & -1 & 0 \\ 0 & C_{e24}/z & C_{e23}/z & 0 & 0 & -1 \end{bmatrix}^{-1} \\ &\begin{bmatrix} C_{ecu21} & 0 & 0 & 0 & 0 \\ C_{ecu31} & 0 & 0 & 0 & 0 \\ 0 & 0 & C_{v21} & 0 & C_{v22} \\ 0 & 0 & C_{v31} & 0 & C_{v32} \\ 0 & C_{e11} & 0 & C_{e12} & 0 \\ 0 & C_{e21} & 0 & C_{e21} & 0 \end{bmatrix} \\ &+ \begin{bmatrix} 0 & 0 & C_{v11} & 0 & C_{v12} \\ C_{ecu11} & 0 & 0 & 0 & 0 \end{bmatrix} \end{aligned} \tag{18}$$

In order to solve the above *distribution constraint* numerically, we need to make assumptions regarding the order of polynomial transfer function matrices $\mathbf{C}_{ecu}$, $\mathbf{C}_v$, $\mathbf{C}_e$. Although the most straightforward approach would be to assume all, $\mathbf{C}_{ecu}$, $\mathbf{C}_v$, $\mathbf{C}_e$ are composed of transfer functions of the same order of the centralized controller $\mathbf{C}_{des}$, this may not be preferable, since it increases the numerical burden of the problem substantially. For the application we are considering here our desired controller transfer matrix consists of polynomials of 11^{th} order which means our non-linear optimization problem would have almost 600 design variables and constraints to handle.

A better way to tackle the numerical burden of the distribution problem is to perform some pre-optimization analysis to better understand and simplify the problem. Fig. 6 shows a typical pole zero map of the desired optimal controller, $\mathbf{C}_{des}$, obtained in the previous section as the VCT Component parameters $\tau_{v,a}$ and $\tau_{v,s}$ vary.

As shown in Fig. 6 in the elements of the desired controller transfer function matrix one can observe some stationary poles and zeros as well as varying poles and zeros which can be exploited for the purposes of improving the modularity. The static pole and zero elements can be placed in the ECU and EGO sensor controller while varying poles can be placed in the VCT Controller. Analyzing the pole zero plots carefully for each element we note that swapping the VCT component with another one would only effect the elements C_{11}, C_{12}, C_{13}, C_{14}, C_{15}, C_{23}, C_{25} (due to varying poles, zeros or both similar to shown in Fig. 6 of our desired optimal controller, $\mathbf{C}_{des}$).

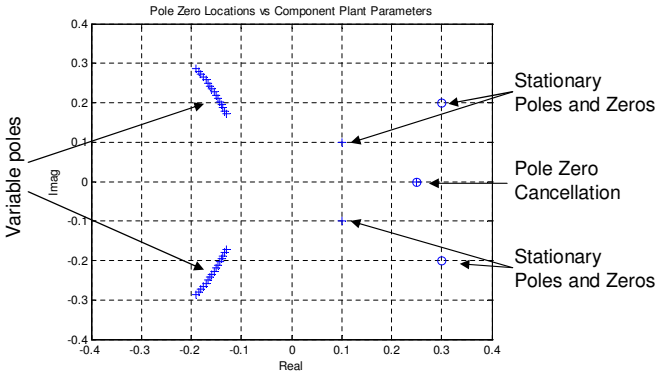

Fig. 6. Simple Pole Zero Map of the $\mathbf{C}_{des}(z)$ as plant variables change.

In order to simplify the numerical optimization problem and obtain a good candidate distribution solution to start the search algorithm we used a two step configuration design process once the Pole-Zero mapping of $\mathbf{C}_{des}(\mathbf{p}_{cs}, \mathbf{p}_v, \mathbf{p}_e, z)$ elements versus the VCT component plant variables, $\mathbf{p}_v$ is obtained:

1) Identify proper transfer functions $C^s_{des,ij}(z)$ and $C^v_{des,ij}(z)$ such that $C_{des,ij}(z) = C^s_{des,ij}(z)C^v_{des,ij}(z)$,
2) Find $\mathbf{C}_{ecu}(z)$, $\mathbf{C}_v(z)$ (with kth row lth column element denoted as $C_{v,kl}(z)$) , $\mathbf{C}_e(z)$ satisfying (a) and (b):
   a) $\mathbf{C}_{dist}(\mathbf{C}_{ecu}, \mathbf{C}_v, \mathbf{C}_e, z)$ is equal to $\mathbf{C}_{des}(\mathbf{p}_{cs}, \mathbf{p}_v, \mathbf{p}_e, z)$
   b) For all $C^v_{des,ij}(z)$ (identified in Step 2) there exists $C_{v,kl}(z)$ such that $C_{dist,ij} = C^s_{des,ij}(z)C_{v,kl}(z)$. Therefore $C_{v,kl}(z)$ can be picked to be $C^v_{des,ij}(z)$ for different VCT components.

The superscript "s" denotes the stationary pole/zero pairs that do not change as $\tau_{v,a}$ and/or $\tau_{v,s}$ change while the superscript "v" denotes those that do vary. It is important to note that the primary goal of this procedure is to place varying poles and zeros to the target component controller while satisfying the distribution constraint in Step $2(a)$. Therefore, it is still acceptable if there are cases where some or all of the stationary poles/zeros reside (e.g., EGO sensor controller as shown in Table II) to satisfy the distribution constraint in Step $2(a)$. The pre-optimization method described above is generic. However, the results (i.e., number of pole zero cancellations, identifying stationary transfer function matrix elements and/or poles and zeros in these elements) would change from one application to another.

Based on the procedure given above, we obtained a candidate solution that maximizes VCT component modularity as shown in Table I. Implementation of this distribution would result in an overall controller:

$$\mathbf{C}_{dist} = \begin{bmatrix} C_{v13}C_{ecu21} & C_{v14}C_{e21} & C_{v11} \\ C_{ecu11} & C_{ecu12}C_{e11} & C_{ecu13}C_{v31}/z \\ & C_{v14}C_{e22} & C_{v12} \\ & C_{ecu12}C_{e12} & C_{ecu13}C_{v32}/z \end{bmatrix} \quad (19)$$

Element	Solution	Element	Solution
C_{ecu11}	C_{21}	C_{ecu12}	1
C_{ecu13}	C^s_{23}/z	C_{ecu21}	C^s_{11}
C_{v11}	C_{13}	C_{v12}	C_{15}
C_{v13}	C^v_{11}	C_{v14}	C^v_{14}
C_{v31}	C^v_{23}	C_{v32}	C^v_{25}
C_{e11}	C_{22}	C_{e12}	C_{24}
C_{e21}	C^s_{12}	C_{e22}	C^s_{14}

TABLE I
TRANSFER FUNCTIONS FOR THE MODULAR VCT CONTROLLER SOLUTION

Element	Solution	Element	Solution
C_{ecu11}	C_{21}	C_{ecu12}	1
C_{ecu13}	1	C_{ecu31}	C^s_{11}
C_{v11}	C_{13}	C_{v12}	C_{15}
C_{v14}	1	C_{v31}	$C_{23}z$
C_{v32}	$C_{25}z$	C_{e11}	C_{22}
C_{e13}	C_{24}	C_{e21}	$C^s_{12}C^v_{12}$
C_{e22}	C_{14}	C_{e24}	$C^d_{11}z$

TABLE II
TRANSFER FUNCTIONS FOR THE MODULAR EGO CONTROLLER SOLUTION

The closed-loop response of this solution is virtually indistinguishable from the overall controller response presented in Fig. 3. The solution for the optimization problem to maximize VCT component modularity (i.e parameters for $\mathbf{C}_{ecu}$, $\mathbf{C}_v$, $\mathbf{C}_e$ transfer function matrices) is the same as the candidate solution as presented in Table I. The numerical value of M^*_v is $60 * 10 = 600(ms)^2$. An interpretation of this number can be given as follows: Assuming the default configuration for other components, optimal controllers can be obtained by only adjusting VCT component controller for VCT plant parameters changing in the ranges $\tau_{v,a} = [7, 67]$ms and $\tau_{v,s} = [10, 20]$ms.

The same steps can also be followed to obtain a candidate solution to maximize EGO sensor modularity: After a similar pole/zero analysis to the one shown in Fig. 6, we have identified only C_{11} and C_{12} elements have varying elements as the EGO sensor changes. By applying the pre-optimization procedure the candidate solution is obtained. As in the VCT case, closed loop response of this solution is virtually indistinguishable from the overall controller response presented in Fig. 3. Since our static pole/zero numerical threshold is within the distribution constraint limits in the optimization problem our candidate solution (Table II) is verified as the optimal distribution which results in $M^*_e = 60ms$ (i.e. given the default configuration, optimal controllers can be obtained by only changing EGO controller in the range $\tau_e = [40, 100]$ms).

IV. Conclusion

In this paper, a method to distribute the discrete MIMO controller for the VCT engine to improve the component swapping modularity of the VCT actuator and the EGO sensor components is presented. This work is an extension of the method described in [3], [4] to a discrete MIMO controller applied to a more complex system. In Section II-C, a discrete LQG controller was designed based on the work from [13]. In Section III-B, this controller was distributed to ECU, a VCT controller and an EGO sensor controller in order to improve the component swapping modularity of the system. In Section III-B, we also present a control oriented *pre-optimization* technique which simplifies the optimization problem, and which results in shorter computation times to obtain a solution. The pre-optimization method identifies and groups together controller poles/zeros which change, or remain unchanged, as the VCT or EGO parameters vary. A candidate solution was devised and used in the optimization problem as the initial solution. Resulting solutions maximizing VCT Component modularity and EGO sensor modularity are given in Tables I and II respectively. The performances of these distributed controllers are indistinguishable from the performance of the original controller as shown in Fig. 3. The range of the obtained solutions depends on stability and properness of the overall controller and distributed controllers as well as the optimization toleration settings.

These distributed controllers provide component-swapping modularity which does not exist in the case of implementing the whole algorithm using a single centralized controller (i.e. using the ECU only). The MIMO controller was designed using a linearized model around a specific operation point. It is expected that the practical implementation of this controller would be done by designing the MIMO controller for various operating points of the VCT engine and then using gain scheduling to calibrate the controller for different operating points. The same schedule oriented approach can be applied to the distributed controller by solving the distribution problem for all of the operating points considered. The minimum component swapping modularity obtained among operating points would then be used for optimization problem purposes.

Future work on this topic will include consideration of VCT and EGO modularity concurrently.

References

[1] K. J. Astrom, "Present developments in control applications," Keynote Paper in IFAC 50th Anniversary Meeting, Heidelberg, 2006.

[2] K. Ulrich and K. Tung, "Fundamentals of product modularity," in *Issues in Design/Manufacture Integration 1991*, A. Sharon, Ed. New York: ASME, 1991, pp. 73–79.

[3] M. Cakmakci and A. G. Ulsoy, "Networked control systems with bi-directional communication among "smart" components," in *Proceedings of the American Control Conference*, Portland, Oregon, June 2005.

[4] ——, "Improving component swapping modularity using bi-directional communication in networked control systems," in *Proceedings of International Symposium on Flexible Automation*, Osaka, Japan, July 2006.

[5] A. Stefanopoulou, J. Cook, J. Grizzle, and J. Freudenberg, "Control-Oriented Model of a Dual Equal Variable Cam Timing Spark Ignition Engine," *ASME Journal of Dynamic Systems, Measurement and Control*, vol. 120, pp. 257–266, 1998.

[6] A. C. Elrod and M. T. Nelson, "Development of variable valve timing engine to eliminate the pumping losses associated with throttled operation." *SAE Paper No. 860537*, 1986.

[7] C. GRAY, "A review of variable engine valve timing," *SAE transactions*, vol. 97, pp. 631–641, 1989.

[8] T. Ma, "Effect of variable engine valve timing on fuel economy," *Society of Automotive Engineers international congress and exposition*, vol. 29, 1988.

[9] G. Meacham, "Variable Cam Timing as An Emission Control Tool," 1970.

[10] R. Stein, K. Galietti, and T. Leone, "Dual Equal Vct–A Variable Camshaft Timing Strategy for Improved Fuel Economy and Emissions," 1995.

[11] H. Lenz and K. Wichart, "Variable valve timing-a possibility to control engine load without throttle," 1988.

[12] R. Steinberg, I. Lenz, G. Koehnlein, M. Scheidt, T. Saupe, and W. Buchinger, "A Fully Continuous Variable Cam Timing Concept for Intake and Exhaust Phasing," 1998.

[13] A. Stefanopoulou, "Modeling and control of advanced technology engines," Ph.D. dissertation, University of Michigan, 1996.

[14] B. Powell and J. Cook, "Nonlinear low frequency phenomenological engine modeling and analysis," *Control Conference, American*, vol. 24, 1982.

[15] A. Stefanopoulou, J. Freudenberg, and J. Grizzle, "Variable camshaft timing engine control," *Control Systems Technology, IEEE Transactions on*, vol. 8, no. 1, pp. 23–34, 2000.